SCEC Report: Using foraminifera to identify co-seismic subsidence along the San Andreas Fault beneath Tomales Bay

ABSTRACT

As much as 43 cm of co-seismic subsidence occurred in upper Tomales Bay, California during the 1906 San Francisco Earthquake. This nearly 0.5 m of subsidence suggests the stratigraphy within the bay may contain a record of past earthquakes along the northern San Andreas Fault. As part of earlier work, we created a foraminifera-based transfer function for identifying past periods of co-seismic subsidence and collected 36 cores in Tomales Bay. The purpose of this work was to foraminifera and sedimentological changes within the upper reaches of Tomales Bay to produce a record of past earthquakes along the northern San Andreas Fault. To accomplish these objectives, we proposed to 1.) create a foraminifera transfer function for Tomales Bay using the distribution of extant foraminifera, 2.) apply the transfer function across sedimentological contacts in cores to test for submergence and 3.) acquire radiocarbon ages across potential co-seismic subsidence events. From our work we have 1.) created a foraminiferal transfer function, 2.) identified 5 possible co-seismic, and 3.) used a hierarchical cluster model to compare our ages along with other studies along the northern San Andreas Fault to provide a better statistical evaluation of through going ruptures along the San Andreas Fault. We confirm an ~300 year return interval for earthquakes since 1300 AD but find a potential change in earthquake frequency prior to that with a possible fourth earthquake at 1200 AD.

Introduction and Rationale

Earthquakes within the San Francisco region put at risk nearly 7 million people (https://earthquake.usgs.gov/earthquakes/events/1868calif/virtualtour/modern.php; last accessed May 14, 2019). The largest historical earthquake to impact this region was the 1906 San Francisco Earthquake, which resulted from a 470-km long rupture of the northern San Andreas Fault. This moment magnitude 7.9 Earthquake (Song et al., 2008) and its accompanying fire resulted in over 3,000 deaths (Hansen and Condon, 1989) and $400 million+ of property damage across northern California (NOAA, 1972). Serious damage from the earthquake was experienced as far north as Humboldt County, California (Dengler, 2008). Recent compilations suggest that the probability of a >6.7 Magnitude Earthquake occurring between 2014 and 2043 along the San Francisco sections of the San Andreas Fault is 22% (Aagaard et al., 2016). However, these estimates are based in part on the study of past earthquake frequency (Schwartz et al., 2014).

Paleoseismic studies suggest that the 1906 Earthquake is a recurring threat across the Bay area. These studies have relied on trenching (Schwartz et al., 1998; Zhang et al., 2006; Kelson et al., 2006; Hall and Niemi, 2008; Streig et al., 2014), offshore studies of turbidites (Goldfinger et al., 2007), and in one record, co-seismic subsidence of a pair of estuaries (Knudsen et al., 2002). Based on this work, it appears that the recurrence interval of events similar to the 1906 Earthquake is around 200-250 years (Niemi and Hall, 1992; Zhang et al., 2006; Goldfinger et al., 2007). However, with the exception of one trench study at Vedanta Marsh (Zhang et al., 2006) and the turbidite record (Goldfinger et al., 2007), this recurrence interval is based only on the time since the last 1906-like earthquake (Schwartz et al., 2014) or the total magnitude of slip over a period of time divided by the slip experienced during the 1906 Earthquake (Niemi and Hall, 1992). Thus, although other late Holocene earthquakes have been documented, only the penultimate earthquake (mid 1600s AD) has been firmly correlated across multiple sites on the northern San Andreas Fault Zone (Schwartz et al., 2014). More paleoseismic studies extending back into the middle to late Holocene are needed to adequately establish recurrence intervals for earthquakes along the northern San Andreas Fault and to test the use of the turbidite record in documenting past earthquakes.

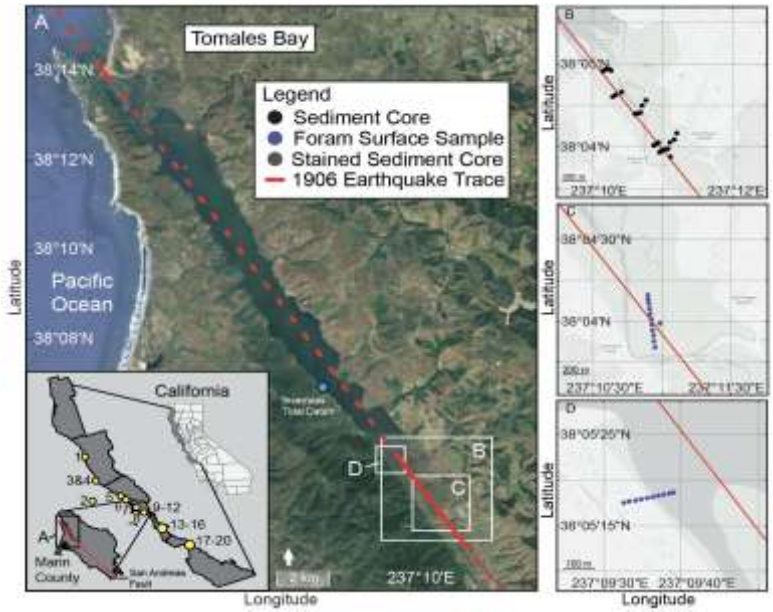

Figure 1. Map of Tomales Bay (A) including the locations of collected sediment cores (B), sediment surface samples (C & D), the Inverness tidal datum, and past paleoseismic study locations of the Northen SAF.

Although motion along the San Andreas Fault is predominately strike-slip, local areas, likely along pull-apart type basins and areas undergoing liquefaction, within Tomales Bay experienced as much as 43 cm of subsidence during the 1906 Earthquake (Lawson, 1908) and neighboring Bolinas Lagoon experienced up to 30 cm of subsidence (Lawson, 1908; Bergquist, 1978; Knudsen et al., 2002). Historic subsidence within the bays and marshes within the San Andreas Fault Zone suggests their deposits likely record past earthquakes (Bergquist, 1978; Knudsen et al., 2002). Studies of lagoon deposits by Bergquist (1978) and Knudsen et al. (2002) found not only evidence for subsidence within Bolinas Lagoon during the 1906 Earthquake but also evidence for two older earthquakes. These older earthquakes date to 400 and 700 years ago (Knudsen et al., 2002). Do the marshes of nearby Tomales Bay also record past earthquakes? Unfortunately since the 1906 earthquake the marshes within the upper reaches of Tomales Bay were filled and diked for cattle ranching and subsequently restored via scrapping in 2009. However, the scrapping was only of the upper <1 m, leaving the older section largely undisturbed, possibly preserving a record of mid to late Holocene earthquakes.

Activities/Methods

Over the course of the past year, we further refined our facies descriptions, collected 8 more sediment cores, counted more foraminifera across sedimentary contacts and obtained 20 new radiocarbon ages. We also presented our results at 2 conferences including the SCEC Annual Meeting in September. The other conference was the GSA Annual Meeting in San Antonio in September of 2025. We also submitted our results for publication in a peer-reviewed journal.

Results/Findings

Sedimentary Facies

Seven sedimentary facies were identified within the cores collected including: an organic-rich grey mud (ORM) facies, organic-poor grey mud (OPM) facies, modeled organic mud facies, interlaminated mud facies, red sand facies, coarse sand facies, and a grey well-sorted sand facies. The ORM facies (2.5Y 3/1) consist of a light to dark grey unconsolidated silty mud. This facies contains gastropods (*nassarius mendicus* and *cerithideopsis californica*) and bivalves (*cryptomya californica* and *haminoea virescens*), throughout the facies in most occurrences. The grey mud facies contains little to no organic material over 1mm in size. This facies is composed of 19.3% clay, 80.5% silt, and .1% very fine

sand sized grains. The OPM facies (2.5Y 3/1) also consist of a light to dark grey unconsolidated silty mud, and contain cm scale sections of preserved plant material. This facies can also contain shell fragments, and little to no organic material > 1mm is present outside of the large sections of preserved plant material. The grain size in this facies is equivalent to that of the ORM facies. The modeled organic mud facies consist of a light to dark brown mud (2.5Y 4/2) with plant fragments throughout. No shell material is seen in this facies. This facies is composed of 18.8% clay, 81% silt, and.1% very fine sand sized grains. The interlaminated mud facies consist of 1cm to 5cm laminations of the ORM and modeled organic mud facies. This facies has a combination of 2.5Y 3/1 and 2.5Y 4/2 on the Munell soil color chart, depending on the lamination. The grain sizes of this facies averaged 28.3% clay, and 71.1% silt. The red sand facies consists of reddish brown (5YR 5/4), fine to medium, well-sorted sand. This facies has no shell material and little to no organics. The coarse sand facies consists of light to dark grey (2.5Y 3/1), muddy sand. Grain size ranges from medium to coarse sand, with coarse well-rounded cobbles always present in a muddy matrix. This facies contains little to no organic material, and in some locations shell fragments are present. The grey, well-sorted sand facies (2.5Y 4/1) consists of fine to medium, well sorted sand. In some instances, this facies appears to fine upwards, but always remains consistently well sorted. Little to no organic material is present in this facies, but in some locations shell fragments are present.

Foraminifera Counts and Transfer Function Results

From the sedimentary descriptions, grain size, foraminifera counts, and radiocarbon ages from our 36 cores collected in Tomales Bay, we have identified 5 potential coseismic events at AD 1169-1370, AD 862-710, AD 687-571, AD 56 to BC 277, and BC 1297-1387 (Fig. 2). These potential co-seismic events are seen in the cores as an abrupt contact between the modeled organic mud facies below and the OPM facies above (Fig. 3). Three of the candidate earthquake contacts (Tomales Bay events 2, 3, and 5) can be correlated across two or more sediment cores, suggesting a spatial extent consistent with co-seismic subsidence (Figure 2). However, because analysis of candidate earthquake events began with abrupt lithologic contacts as potential event horizons, it is possible that additional earthquake-related deposits occur elsewhere in the marsh but are not preserved as distinct contacts, leaving the signal masked within a single sedimentary facies. This may also explain why two candidate events (Tomales Bay 1 and 4) were identified in only one core (Figure 2).

We also counted foraminifera across each of these 5 contacts. Tomales Bay event 2 shows the clearest evidence for coseismic subsidence at 47 ± 19 cm of subsidence. Event 3 shows 31 +/- 27 cm of subsidence and event 4 shows 29 +/- 30 cm of possible subsidence. Events 1 and 5 show much less subsidence at 15 +/- 18 cm and 11 +/- 45 cm of possible subsidence across the surfaces, respectively.

Overall, due to the lithologic and ecological evidence present at each of our candidate subsidence events, and comparison with timing of other (a parameter within Nelson et al.'s (1996) synchroneity criteria), we feel confident in our interpretation of co-seismic subsidence for Tomales Bay events 2 and 4. Tomales Bay event 1 also contains a sharp lithologic contain and compares in timing with other sites along the SAF, but its less definitive foraminiferal assemblages and appearance in only one sediment core reduces our confidence in its interpretation as subsidence events. While events 3 and 5 have sharp lithologic contacts and can be correlated across multiple cores, the lack of definitive foraminiferal assemblages reduces our confidence in their interpretation as subsidence events.

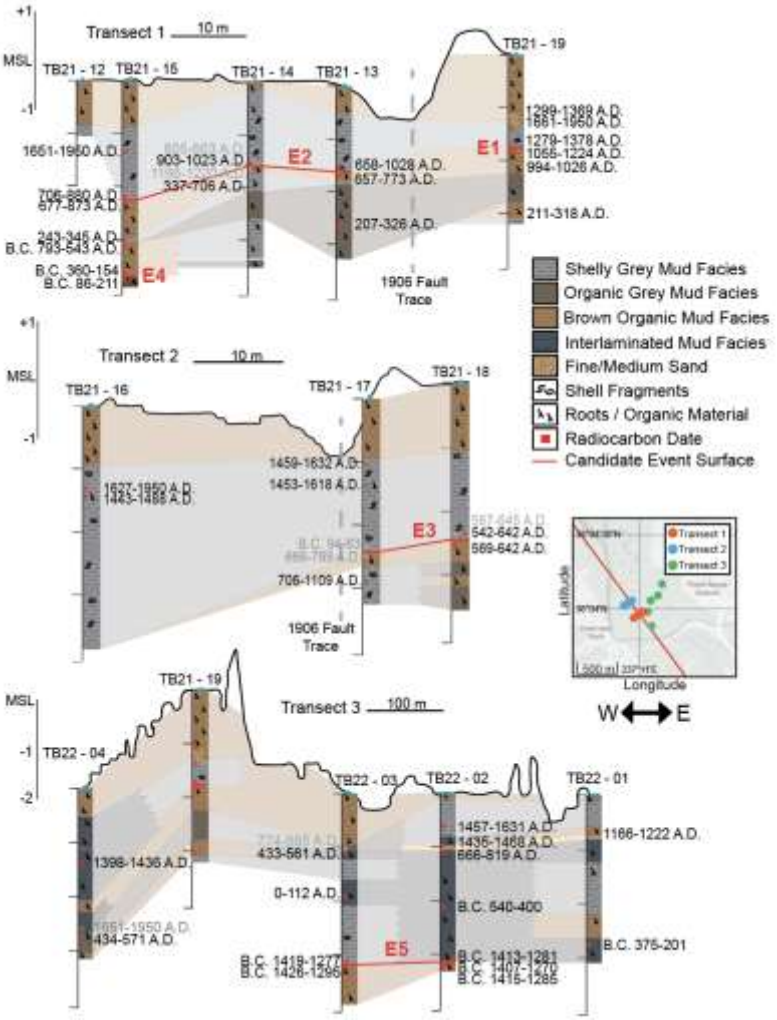

Figure 2. Schematic core description of three core transects, showing the 5 potential subsidence event contacts in red. Calibrated ^{14}C ages (2s ranges) displayed at depth collected. Grey radiocarbon ages represent those removed from the Oxcal age model due to low agreement (A < 60%).

Comparison with other earthquake records

We used a hierarchical cluster model and dendrogram to compare our new results with the ages of potential earthquakes found in other studies (Fig. 3). The hierarchical cluster model from the studies summarized identified 15 total potential earthquakes clusters; however, not all are likely to be separate events as some clusters (e.g. 6, 10, etc.) overlap in age with several other cluster but define events reported in the literature with age error bars too large to assign to a specific other cluster. Additionally, some are only found in one record and may record only local events. However, five of these clusters (1,3, 5, 8, and 10), two of which contain earthquakes found in Tomales Bay, contain three or more earthquake ruptures and likely represent through going events on the San Andreas Fault. Additionally, some of the older events (11, 13, 14, and 15) may be more widespread but are only found in the limited records preceding 500 AD (Fig. 3), one, event 15 at 1297-1387 BC, is new to this study. The new cluster analysis suggests that the 300-year recurrence interval might only apply to the last 3 events (inclusive of the 1906 earthquake), with a potential change in recurrence prior to 1300 AD.

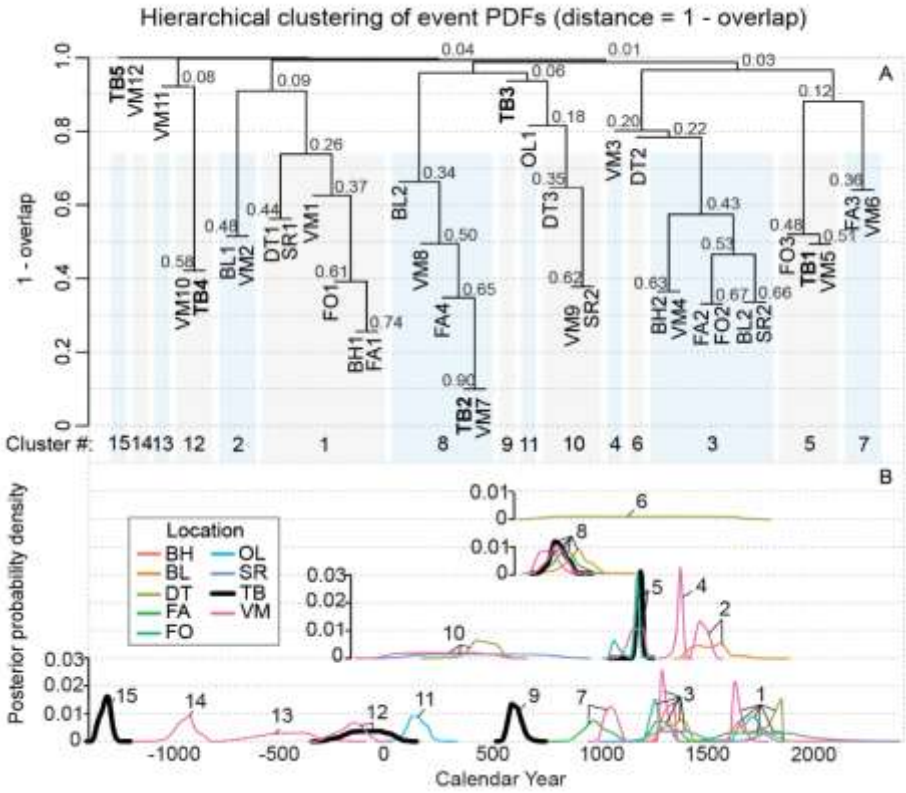

Figure 3. A) Hierarchical clustering dendrogram of earthquake event PDFs from multiple locations. Pairwise similarity between event PDFs was quantified as the integral of their overlap (0= no overlap, 1 = complete overlap). Distances for clustering are defined as 1-overlap, so branches that join at lower heights indicate events with greater similarity in their age probability distributions. The y-axis shows this distance metric, which the x-axis lists individual events-location PDFs, and shows the cluster they are assigned to using a 26% similarity cutoff. B) PDFs for each earthquake event recorded along the North Coast segment, colored by location. Tiering of clusters is done to more clearly see cluster overlap. Numbers refer to cluster groups from panel A. BH - Bodega Harbor; BL - Bolinas Lagoon; DT - Dogtown; FA - Fort Ross Archae; FO - Fort Ross Orchard; SR - Scaramella Ranch; TB - Tomales Bay; VM - Vedanta Marsh.

Other products resulting from this work

This research comprises 2 chapters of the PhD dissertation of Claire Divola, who is in her final year of a PhD program at UCSB and anticipates graduating in the spring/summer of 2026. The meeting abstracts associated with this work include:

Claire Divola, Alexander R. Simms, and Ed Garrett. (2025). **Using Foraminifera to Identify Earthquakes Along the Northern San Andreas Fault, Tomales Bay, California.** SCEC Annual Meeting, Palm Springs, CA, (Poster)

Claire Divola, Alexander R. Simms, and Ed Garrett. (2025). **A record of earthquakes along the northern San Andreas Fault preserved in the sediments of Tomales Bay, California.** GSA Annual Meeting, San Antonio, Texas. (Talk)

References:

Aagaard, B.T., Blair, J.L., Boatwright, J., Garcia, S.H., Harris, R.A., Michael, A.J., Schwartz, D.P., DiLeo, J.S., 2016. Earthquake outlook for the San Francisco Bay Region 2014-2043. USGS Fact Sheet 3020, 1-6.

Bergquist, J.R., 1978. Depositional history and fault-related studies, Bolinas Lagoon, California. USGS Open File Report 78-802, 1-164.

Dengler, L., 2008. The 1906 Earthquake on California's North Coast. Bulletin of the Seismological Society of America 98, 918-930.

Goldfinger, C., Morey, A.E., Nelson, C.H., Gutierrez-Pastor, J., Johnson, J.E., Karabanov, E., Chaytor, J., Eriksson, A., Party, S.S., 2007. Rupture lenghts and temporal history of significant earthquakes on the offshore and north coast segments of the northern San Andreas Fault based on turbidite stratigraphy. Earth and Planetary Science Letters 254, 9-27.

Hall, N.T., Niemi, T.M., 2008. The 1906 Earthquake fault rupture and paleoseismic investigation of the northern San Andreas Fault at Dogtown Site, Marin County, California. Bulletin of the Seismological Society of America 98, 2191-2208.

Hall, N.T., Wright, R.H., Clahan, K.B., 1999. Paleoseismic studies of the San Francisco Peninsula segment of the San Andreas fault zone near Woodside, California. Journal of Geophysical Research 104, 23,215-223,236.

Hansen, G., Condon, E., 1989. Denial of Disaster. Cameron and Company, San Francisco.

Kelson, K.I., Streig, A.R., Koehler, R.D., Kang, K.-H., 2006. Timing of Late Holocene paleoearthquakes on the northern San Andreas Fault at the Fort Ross Richard Site, Sonoma County, California. Bulletin of the Seismological Society of America 96, 1012-1028.

Knudsen, K.L., Witter, R.C., Garrison-Laney, C.E., Baldwin, J.N., Carver, G.A., 2002. Past earthquake-induced rapid subsidence along the northern San Andreas Fault: a paleoseismological method for investigating strike-slip faults. Bulletin of the Seismological Society of America 92, 2612-2636.

Lawson, A.C., 1908. The California Earthquake of April 18, 1906: Report of the State Earthquake Investigation Commission, Washington D.C., p. 451.

Niemi, T.M., Hall, N.T., 1992. Late Holocene slip rate and recurrence of great earthquakes on the San Andreas fault in northern California. Geology 20, 195-198.

Schwartz, D.P., Lienkaemper, J.J., Hecker, S., Kelson, K.I., Fumal, T.E., Baldwin, J.N., Seitz, G.G., Niemi, T.M., 2014. The earthquake cycle in the San Francisco Bay Region: A.D. 1600-2012. Bulletin of the Seismological Society of America 104, 1299-1328.

Schwartz, D.P., Pantosti, D., Okumura, K., Powers, T.J., Hamilton, J.C., 1998. Paleoseismic investigations in the Santa Cruz mountains, California: Implications for recurrence of large-magnitude earthquakes on the San Andreas fault. Journal of Geophysical Research 103, 17,985-918,001.

Shennan, I., Garrett, E., Barlow, N., 2016. Detection limits of tidal-wetland sequences to identify variable rupture modes of megathrust earthquakes. Quaternary Science Reviews 150, 1-30.

Song, S., Beroza, G.C., Segall, P., 2008. A unified source model for the 1906 San Francisco earthquake. Bulletin of the Seismological Society of America 98, 823-831.

Streig, A.R., Dawson, T.E., Weldon, R.J.I., 2014. Paleoseismic evidence of the 1890 and 1838 Earthquakes on the Santa Cruz Mountains Section of the San Andreas Fault, near Corralitos, California. Bulletin of the Seismological Society of America 104, 285-300.

Zhang, H., Niemi, T., Fumal, T., 2006. A 3,000-year record of earthquakes on the northern San Andreas Fault at the Vendanta Marsh Site, Olema, California. Seismological Research Letters 77, 248.